JACS Au
AN OPEN ACCESS JOURNAL OF THE AMERICAN CHEMICAL SOCIETY

pubs.acs.org/jacsau

Article

Synthetic Control of Mitochondrial Dynamics: Developing Three-Coordinate Au(I) Probes for Perturbation of Mitochondria Structure and Function

R. Tyler Mertens, William C. Jennings, Samuel Ofori, Jong Hyun Kim, Sean Parkin, Gunnar F. Kwakye, and Samuel G. Awuah*

Cite This: https://dx.doi.org/10.1021/jacsau.1c00051

Read Online

ACCESS | Metrics & More | Article Recommendations | Supporting Information

ABSTRACT: Mitochondrial structure and organization is integral to maintaining mitochondrial homeostasis and an emerging biological target in aging, inflammation, neurodegeneration, and cancer. The study of mitochondrial structure and its functional implications remains challenging in part because of the lack of available tools for direct engagement, particularly in a disease setting. Here, we report a gold-based approach to perturb mitochondrial structure in cancer cells. Specifically, the design and synthesis of a series of tricoordinate Au(I) complexes with systematic modifications to group 15 nonmetallic ligands establish structure−activity relationships (SAR) to identify physiologically relevant tools for mitochondrial perturbation. The optimized compound, **AuTri-9** selectively disrupts breast cancer mitochondrial structure rapidly as observed by transmission electron microscopy with attendant effects on fusion and fission proteins. This phenomenon triggers severe depolarization of the mitochondrial membrane in cancer cells. The high in vivo tolerability of **AuTri-9** in mice demonstrates its preclinical utility. This work provides a basis for rational design of gold-based agents to control mitochondrial structure and dynamics.

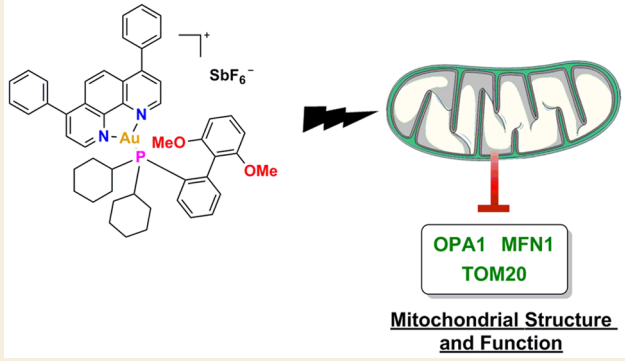

KEYWORDS: *mitochondria, gold compounds, chemical probe, structure, anticancer, breast cancer, biogenesis*

Mitochondria are dynamic organelles that control ATP production, biosynthesis of macromolecules, and signaling. Often referred to as the powerhouse of the cell, the mitochondria have a well-defined but complicated structure with important functional implications. The outer membrane envelops the inner-membrane energy hub, which protects a dense protein-rich matrix.[1] The large surface area of the inner membrane is characterized by a macromolecular folding, known as *cristae*. There exists an intimate relationship between mitochondria morphology and cellular bioenergetics.[2] A key dynamic parameter of regulated mitochondria function is fusion and fission.[3] A balanced cycle of fusion and fission is critical for physiology and the loss thereof has adverse implications on cell function, leading to inflammation, aging, neurodegeneration, and cancer (Figure 1).[4,5] Thus, tools to study mitochondrial structure is an unmet need and an attractive approach for developing new therapeutics.

As part of a large research program in our laboratory to develop mitochondrial probes and targeting approaches, we are particularly interested in the synthetic control of mitochondrial homeostasis. We recently reported the development of gold agents, which have interactions with the mitochondrial OXPHOS machinery and cellular metabolism. We and others

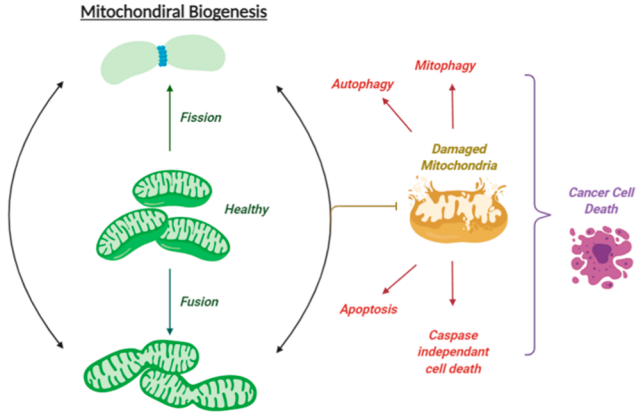

Figure 1. Mitochondrial biogenesis is a key component in maintaining cell homeostasis.

Received: February 8, 2021

have shown that gold compounds can be tuned for mitochondrial localization.[6] Increasing evidence suggests that mitochondrial biological processes participate in acquired drug resistance. Specifically, loss of the mitochondrial protein CLPB compromises mitochondrial structural and functional integrity leading to AML sensitization to apoptosis.[7] Thus, we envisioned that developing small-molecules to disrupt mitochondrial structure will be of therapeutic benefit. However, synthetic alteration of oxidation states or ligand environment of gold compounds for direct mitochondria interaction or targeting of distinct locales is unknown.

The development of gold-based small-molecules for biological use received a major boost following the FDA approval of auranofin for the treatment of rheumatoid arthritis.[8] Over the past decade, several gold compounds have been synthesized as potential therapeutic agents for a plethora of diseases.[9−13] Their unique properties have alluded to unique behavior both in vivo and in vitro in comparison to other transition metal-based alternatives.[14−19] Despite the breadth of gold complex libraries developed thus far, the unique geometry of tricoordinated Au(I) complexes[20−25] are uncommon and their therapeutic potential left untapped.[26−28] Bourrisou and co-workers have demonstrated catalytic capability with tricoordinate complexes due to their distinct reactivity.[27,29−32] We sought to explore the effect of these geometrically unique gold complexes on mitochondria morphology and functional consequences in normal or cancerous epithelial cells.

Our approach included the diversification of compounds using different N^N-bidentate ligands to tune lipophilicity and monodentate arsine or phosphine ancillary ligands to define a unique degree of asymmetry for interaction with biomolecules in a manner distinct from other transition metal complexes. The SAR enabled the selection of a potent candidate that rapidly perturbed the structure of mitochondria after 1 h as observed using transmission electron microscopy. The phenotype observed was sharply different from other agents of known mode of action. Additionally, immunoblotting, respirometry, and quantitative proteomics studies corroborate the discovery of a novel gold compound with specificity for mitochondrial structure. We explored the anticancer potential of the compounds and found that they possess an appreciable selectivity to kill cancer cells compared to normal ones. Preliminary toxicity studies in mice demonstrate that **AuTri-9** can be tolerated safely at 10 mg/kg, highlighting the potential of metal-based compounds for mitochondrial biology.

RESULTS AND DISCUSSION

Rationale, Synthesis, and Characterization of AuTri Complexes

The quest to develop chemical tools that target distinct aspects of the mitochondrion prompted investigations into reagents that can perturb mitochondrial structure. Given previous reports in the literature of cationic gold complexes directly affecting mitochondrial damage and mitochondrial permeabilization,[33−40] we were intrigued to see the effect of cationic tricoordinate complexes in mitochondrial biological systems. Tricoordinate compounds can assume an unsymmetrical structure with one longer metal-heteroatom bond length, which is weak enough to act as a coordination site upon bond breakage. This deviation from the use of leaving groups bonded to metal centers was the motivation for our work. We hypothesized that unsymmetrical gold compounds would provide a distinct labile character to interact with biomolecules (vide infra). Therefore, we designed and synthesized a class of novel compounds to enable SAR studies. Tricoordinate gold(I) complexes were achieved by a facile synthetic protocol (Scheme 1). Commercially available phosphine and arsine

Scheme 1. Facile Synthesis of Novel Tricoordinate Gold(I) Complexes with SAR

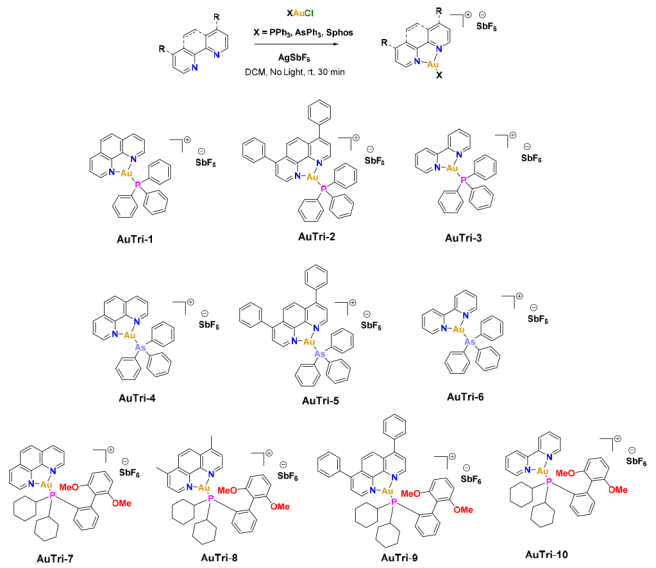

ligands were treated with either $HAuCl_4{\cdot}3H_2O$ or AuCl(tht) to afford the neutral gold(I) precursors. These precursors were subjected to silver transmetalation by adding to a suspension of the gold(I) pecursor in dichloromethane, the corresponding silver salt, and N^N bidentate ligand of choice to afford a library of cationic tricoordinate gold(I) complexes **AuTri-1−10** in good-to-excellent yields (Supporting Information). The synthetic feasibility allows for a vast library of complexes to be developed in a short amount of time.

X-ray Crystallography

To further elucidate the unique geometry, the structures of six complexes were solved by X-ray diffraction techniques. Structure of **AuTri-6** (Figure 2a) demonstrates a clearly

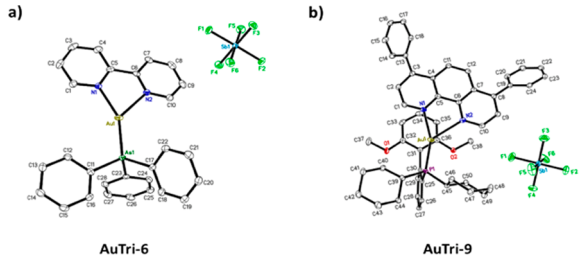

Figure 2. X-ray crystal structures: (a) structure of **AuTri-6** and (b) structure of **AuTri-9**. Outer-sphere solvent molecules are omitted for clarity. Thermal ellipsoids are shown at the 50% probability level.

unsymmetrical three coordinate geometry around the gold center. The N^N-bidentate ligand shows heavy distortion with one Au−N bond length significantly longer than the other as exemplified by compound **AuTri-6** (Au1−N1 = 2.187(2) Å and Au1−N2 = 2.374(2) Å). Consequently, the bite angle between N1−Au−N2 (71.89°(9)) is significantly smaller than

https://dx.doi.org/10.1021/jacsau.1c00051
JACS Au XXXX, XXX, XXX−XXX

observed in gold(III) phenanthroline complexes, which are typically between 81 and 83°.[41] Additionally, we were able to confirm the structure of our lead compound, **AuTri-9**, with the help of X-ray crystallography (Figure 2b). Again, the symmetric distortion between Au−N bonds can be observed with Au−N1 (2.1636(17) Å) and Au−N2 (2.5046(17) Å). All further crystallographic parameters, as well as structures, for complexes **AuTri-4**, **AuTri-8**, and **AuTri-10** can be found in the Supporting Information. We propose that the unique geometry of these complexes would impart unexplored reactivity in vivo in comparison to the typical linear d^{10} gold complexes.

In Vitro Cell Viability

Once we had established a library of the tricoordinate gold(I) complexes, we then explored their anticancer efficacy in vitro by initially testing the complexes in a cisplatin resistant breast cancer cell line, MDA-MB-231 (Table 1). Over 50% of cancer patients worldwide receive some type of platinum based drug.[42]

Table 1. Cell Viability of All Ten Complexes in TNBC Cell Line MDA-MB-231 Using MTT Assay[a]

MDA-MB-231	
compound	IC_{50} value (μM)
AuTri-1	8.65 ± 0.122
AuTri-2	2.51 ± 0.151
AuTri-3	6.56 ± 0.354
AuTri-4	3.98 ± 0.359
AuTri-5	0.825 ± 0.065
AuTri-6	11.75 ± 0.492
AuTri-7	5.41 ± 0.245
AuTri-8	1.12 ± 0.095
AuTri-9	**0.501 ± 0.03**
AuTri-10	4.65 ± 0.423
1,10-phenantrholine	7.21 ± 1.68
4,7-dimethylphenanthroline	14.08 ± 2.58
bathophenanthroline	7.48 ± 1.64
bipyridine	17.54 ± 0.354
cisplatin	34.56 ± 0.783
auranofin	1.31 ± 0.15
NaSbF6	>50

[a]Cells were incubated with the compounds for 72 h. All compounds were added from stock solutions at a DMSO concentration <1%. Data are represented as the mean ± s.e.m., n = 3.

These drugs have been used to treat testicular, ovarian, cervical, and non-small-cell lung cancers effectively. However, the success of these drugs are limited by resistance from long exposure times to the drugs.[43] Moreover, platinum-based drugs have been used in breast cancer cell lines such as BRCA-1 deficient and triple negative breast cancer (TNBC) cell lines; however, their efficacy is short-lived due to resistance from alteration to multiple cellular pathways.[44,45] With this in mind, our initial screening of the tricoordinate complexes in MDA-MB-231 proved to be a crucial first step in evaluating the cellular toxicity. All the compounds were more cytotoxic in MDA-MB-231 cells in comparison to cisplatin (IC_{50} = 34.56 ± 0.783 μM, Table 1). Next, we evaluated cellular selectivity by testing the ten complexes in MRC5, a normal lung fibroblast cell line (Figure 3a). Interestingly, these complexes all exhibited IC_{50} values over 50 μM. This selectivity is key, as toxicity to healthy cells is a main source of harmful side effects with regards to traditional platinum based chemotherapeutics. Overall, complexes bearing the Sphos ancillary ligand (i.e., **AuTri-7−10**) were more effective than PPh_3 and $AsPh_3$. To establish that the observed cytotoxicity was due to the gold(I) complex itself and not the bidentate framework, all four bidentate ligands were evaluated in MDA-MB-231. The cytotoxicity of the ligands were ≥7 μM (Table 1), indicating that the observed cytotoxicity of the AuTri complexes is not attributed solely to the bidentate backbone. We, then, evaluated the effect of the SbF_6^- counterion. Common counterions used in biologically relevant transition metal complexes are BF_4^- and the most common being PF_6^-. We used $NaSbF_6$ as the source of the counterion, and to our delight, there was no cytotoxicity observed (IC_{50} > 50 μM, Table 1). Furthermore, SAR considering the different bidentate ligands revealed that the derivatives of bathophenanthroline (bphen) were more toxic than their counterparts (Figure 3b). This is attributed to improved stability and lipophilic character of the bphen ligand. The combined SAR gave us our lead compound, **AuTri-9**, as the most promising candidate moving forward, with an IC_{50} value of 0.501 ± 0.03 μM (Table 1). To evaluate the efficacy of our lead compound further, we compared it to known FDA approved drug, auranofin. Given the observed IC_{50} value of auranofin (1.31 ± 0.15 μM, Table 1), **AuTri-9** proved to be a potent candidate for extensive biological characterization. We then explored the efficacy of **AuTri-9** in an array of cell lines in an attempt to validate the effect across a broad range of cell lines (Figure 3c). **AuTri-9** demonstrated competitive cellular toxicity across a panel of cell lines. Additionally, a comparison of the free ligand (Sphos) and gold(I) precursor (ClAuSphos), reveal that the observed cellular toxicity is a result of the unified **AuTri** complexes and not the ligands (Figure 3d).

Solution Stability and Reactivity

Solution stability of metal complexes is a critical factor in the development of effective transition metal based therapeutics. The longevity of the complex in biological systems determines important parameters including but not limited to cytotoxicity, maximum tolerated doses, and pharmacokinetics. To assess the stability of these gold complexes, we initially subjected them to time dependent stability studies in the biologically relevant media Dubellco modified essential medium (DMEM, see Figure 4a for **AuTri-9**). We monitored changes in the absorption spectra of **AuTri-1−10** over the course of a 24-h time period, incubating the solutions at 37 °C (figures for all complexes **AuTri-1−8,10** can be found in the Supporting Information). We observed that the PPh_3 derivatives were relatively stable over the 24-h period, with the exception of the bpy analogue (**AuTri-3**). The extra electronics of the more conjugated phen and bphen derivatives provide enhanced stability to the gold metal center. Not surprisingly, the $AsPh_3$ analogues were not stable, rapidly reducing to elemental gold after the 12-h mark. The increased bond length observed between Au−As in complexes **AuTri-4−6** confirms the lability of those compounds and may explain their relatively rapid reduction. Complexes **AuTri-7−10** proved to be very stable over the 24-h period due to the stronger Au−P bonds. Our lead compound **AuTri-9**, was exceptionally stable over the 24-h time period (Figure 4a) with no alterations to the UV−vis spectra. We further evaluated the solubility and stability of **AuTri-9** in DMSO (Figure 4b) and PBS (Figure 4c) using

https://dx.doi.org/10.1021/jacsau.1c00051
JACS Au XXXX, XXX, XXX−XXX

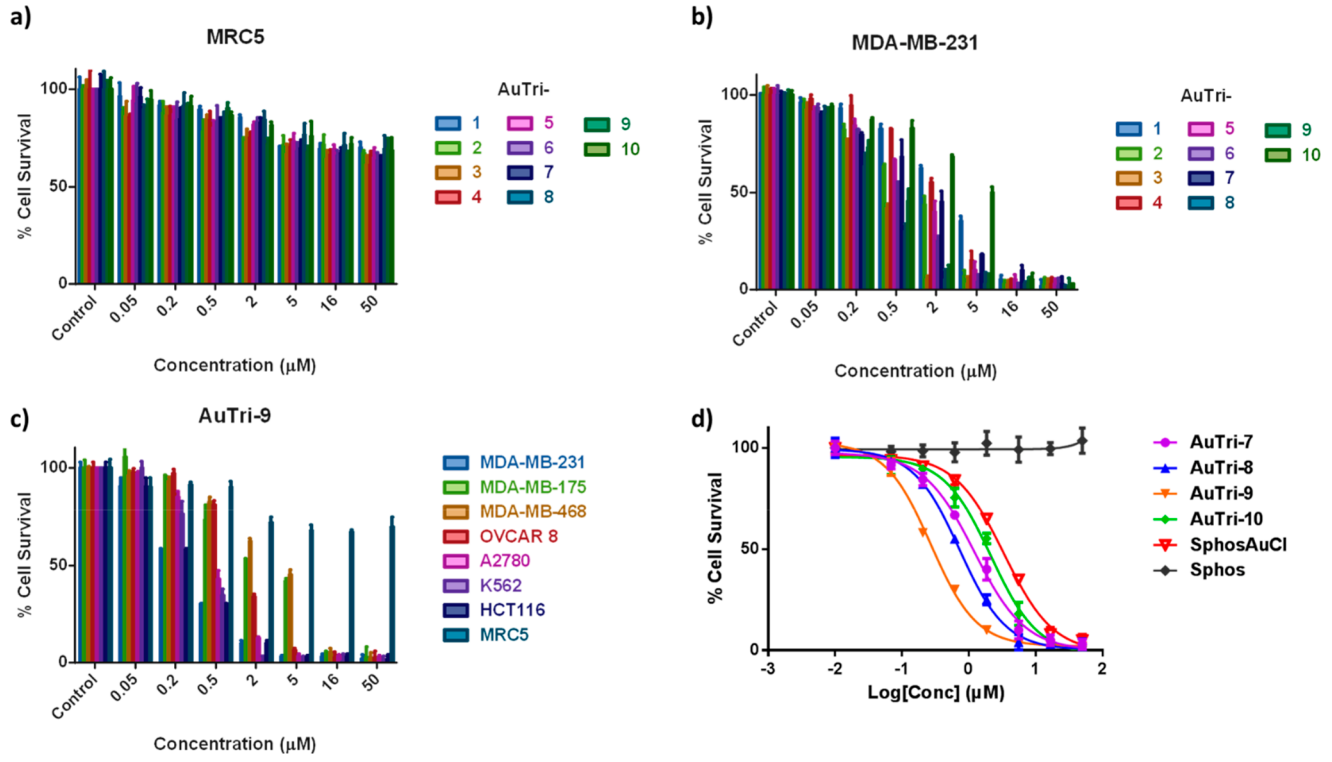

Figure 3. Cell proliferation assays. (a) Cell viability of all 10 complexes in MRC5 over 72 h. (b) Cell viability of Sphos derivatives in MDA-MB-231 over 72 h. (c) Cell viability of **AuTri-9** in a panel of cell lines over 72 h. (d) SAR of Sphos-based derivatives in MDA-MB-231 over 72 h. Control or compounds were treated to ensure a final concentration <1% DMSO. All data are plotted as the mean ± s.e.m., n = 3.

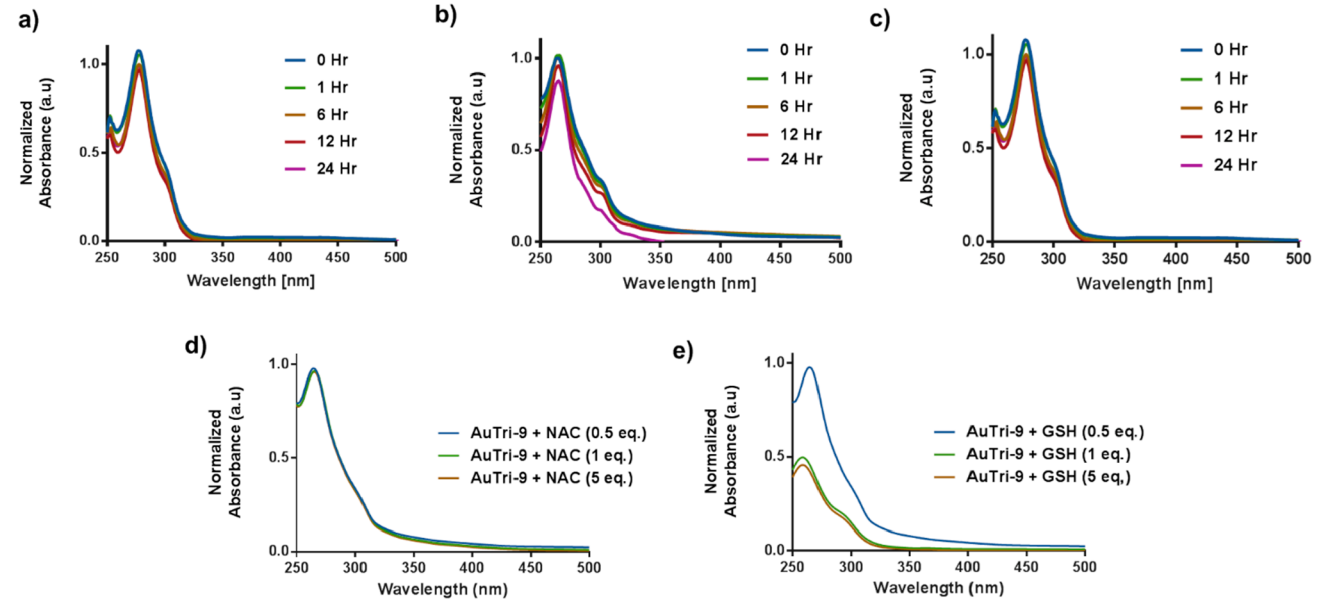

Figure 4. UV−vis assessment of **AuTri-9** stability and reactivity: (a) UV−vis stability of **AuTri-9** (50 μM) in DMEM at 37 °C over 24 h, (b) UV−vis stability of **AuTri-9** (50 μM) in DMSO at 37 °C over 24 h, (c) UV−vis stability of **AuTri-9** (50 μM) in PBS at 37 °C over 24 h, (d) reactivity of **AuTri-9** (50 μM) with NAC at 37 °C over 1 h, and (e) reactivity of **AuTri-9** (50 μM) with GSH at 37 °C over 1 h.

UV−vis spectroscopy. All complexes are readily soluble in both DMSO and MeCN, however; we wanted to evaluate the stability of **AuTri-9** in DMSO and PBS solutions over an extended time period. When evaluated over a 24 h time period, the complex exhibits minimal changes in its absorption profile, indicative of suitable stability and solubility of the compound in solution. Further, we explored the reactivity of **AuTri-9** with common thiol reductants including *N*-acetyl cysteine (NAC) and L-glutathione (GSH). We monitored the reaction by UV−vis spectroscopy. We incubated a PBS solution of **AuTri-9** with both NAC (Figure 4d) or L-GSH (Figure 4e) at varying equivalents over 1 h. The reaction involving NAC did not impact the absorption band of **AuTri-9**, suggestive of no reaction with NAC. Conversely, when **AuTri-9** was exposed to L-GSH, a decrease in the absorbance spectrum was observed, indicating reactivity with this nucleophile. Given that intra-

https://dx.doi.org/10.1021/jacsau.1c00051
JACS Au XXXX, XXX, XXX−XXX

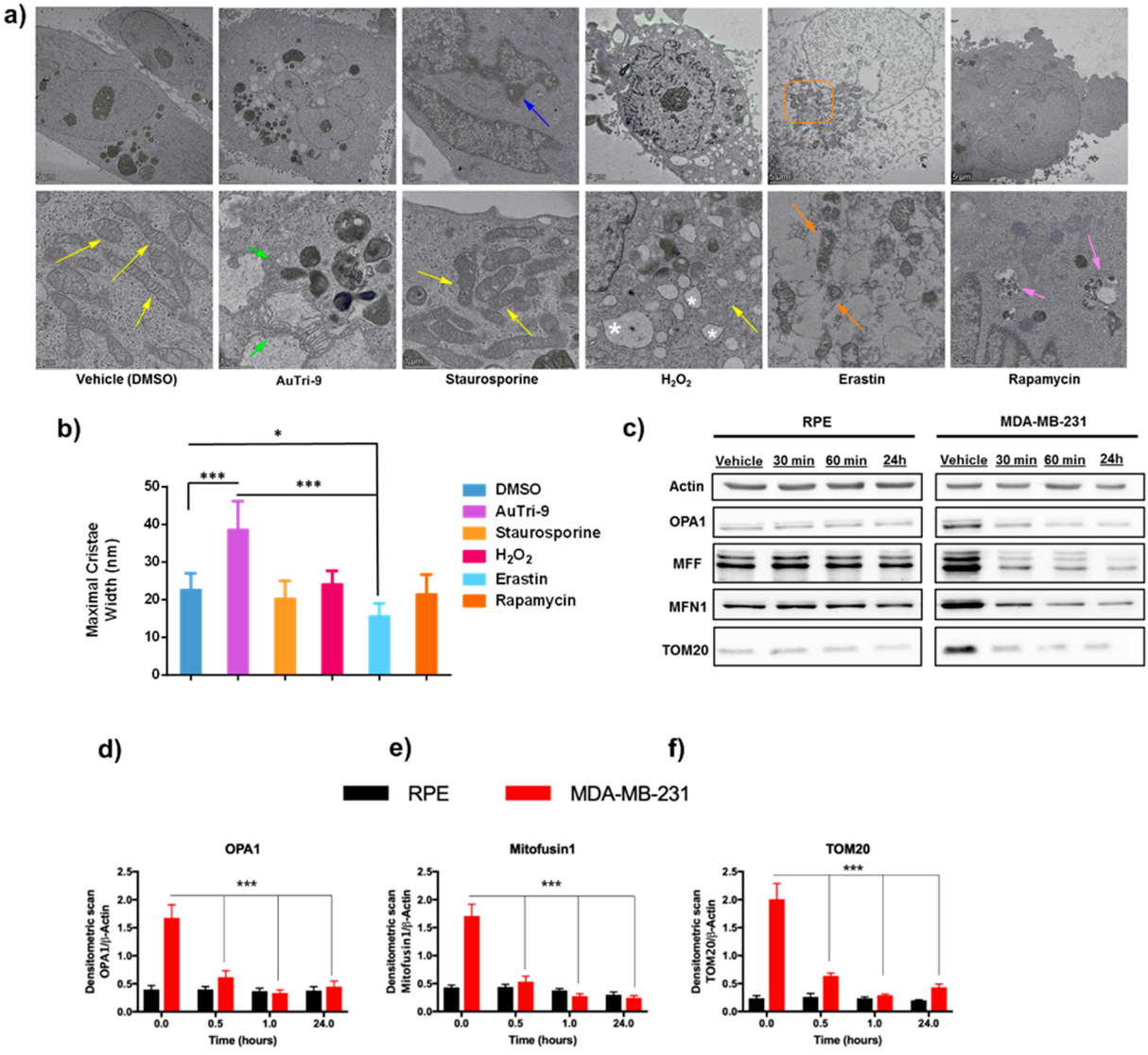

Figure 5. (a) Transmission electron microscopy of known cell death inducers, vehicle control, and **AuTri-9** in MDA-MB-231, 1% DMSO was added to the control wells. Depicted in the panels as follows: healthy mitochondria (yellow arrows), fragmented cristae (green arrow), cytosolic swelling (white star), shrunken mitochondria (orange arrow and orange box), double membrane vesicle (purple arrow). (b) Maximal cristae width. Data are representative of 10 cells chosen at random $n = 10$, where mitochondria were also chosen at random, and a maximum of 3 cristae measured per individual mitochondrion. Total number of cristae measured per each cell, $n = 100$, data are then plotted as mean ± s.e.m. (c) Immunoblots of OPA1, MFF, MFN1, and TOM20. Full blots can be seen in the Supporting Information. (d–f) Representative quantitative protein content of OPA1, MFN1, and TOM20, respectively. $n = 5$, $^{*}p < 0.05$, and $^{***}p < 0.001$.

cellular thiols are common binding targets of gold(I) complexes, this interaction is not surprising. Of note, there was no reduction to elemental gold.

Compound AuTri-9 Directly Affects Mitochondrial Morphology and Structure

To examine the direct effect of the geometrically distinct gold agents on mitochondria, we selected our lead compound, **AuTri-9**. Morphological changes to mitochondria are associated with different cell phenotypes or cell death mechanisms. Targeting mitochondrial processes is a fruitful arena for metallodrug discovery.[36,37,46−48] We employed the use of transmission electron microscopy (TEM) to look at the exact morphological changes in mitochondria of cells exposed to **AuTri-9**. We treated MDA-MB-231 with **AuTri-9**, staurosporine (STS) an apoptosis inducer (e.g., chromatin condensation and margination); hydrogen peroxide, which induces necrosis (e.g., cytoplasmic and organelle swelling, plasma membrane rupture); rapamycin for cellular induced autophagy (e.g., formation of double-membrane enclosed vesicles) and erastin, a known ferroptosis inducer (Figure 5a).[49] When comparing **AuTri-9** with our vehicle control, clear rupture of mitochondrial membranes can be observed along with fragmented cristae (green arrow). Healthy mitochondria (yellow arrow) show distinct intact outer membrane and cristae, thus we suspect that our compound is directly effecting the structure of mitochondria. Comparing **AuTri-9** treatment with H_2O_2, the distinct cytoplasmic swelling and membrane rupture (white star) is observed; however, the mitochondrial structure remains intact. Comparison to erastin showed opposite effects, **AuTri-9** demonstrated fragmentation and destruction of mitochondria structure, whereas erastin showed mitochondrial shrinkage (orange arrow). Furthermore, comparison of mitochondrial features with both rapamycin and

https://dx.doi.org/10.1021/jacsau.1c00051
JACS Au XXXX, XXX, XXX−XXX

staurosporine revealed dissimilar morphological changes. Both rapamycin (yellow arrow) and staurosporine (pink arrow) showed no distinct morphological changes to mitochondria. Mitochondrial cristae play a pivotal role in overall cell health. Under normal biological conditions, mitochondria undergo fusion/fission and cristae form junctions throughout the mitochondria. This allows for the redistribution of cytochrome C from the cristae lumen to the intermembrane space.[50] As earlier noted, mitochondrial bioenergetics and normal mitochondrial structure are crucial to maintaining MMP, the driving force of ATP production. Using Velox digital micrograph software, we measured the cristae width within each treatment condition to quantify and compare the morphological change (Figure 5b). We found that treatment with **AuTri-9** resulted in significantly increased maximal cristae width in comparison to the vehicle control, implicating dysfunctional cristae and decrease in mitochondrial biogenesis. This phenomenon may be exploited to develop therapeutics and study mitochondrial dynamics. Overall, a distinct profile to mitochondrial structure disruption can be achieved in a rapid manner using **AuTri-9**.

To investigate the consequence of mitochondrial structure perturbation, we performed immunoblotting of critical proteins involved in maintaining mitochondrial structure homeostasis. We examined TOM20, a protein located on the outer membrane as a component of the import receptor complex, MFN1, a key protein responsible for mitochondria fission, MFF, a protein primarily responsible for mitochondrial division, and OPA1, a critical protein involved in maintaining mitochondrial structure (Figure 5c).[51−55] Immunoblotting in MDA-MB-231 as well as our normal cell model, RPE, revealed a decrease in protein content of all four structure proteins in MDA-MB-231. Notably, there was no change in protein levels in the healthy cell model. Normalized protein levels confirmed the noted changes (Figures 5d−f). It is worth noting that rapid protein changes were observed within 30 min of treatment. The downregulation of OPA1 by immunoblotting and quantitative proteomics, suggests that this protein is a potential direct target of **AuTri-9**. Recently, a study demonstrated that in HeLa cells, loss of OPA1 leads to fragmentation of the mitochondrial network in conjunction with loss of mitochondrial membrane potential thus causing fragmentation and disorganization of mitochondrial cristae, which resulted in caspase-dependent apoptotic death. With this knowledge, we can state that disruption of mitochondrial structure is just as pertinent to cell homeostasis as any other biological system.

Compound AuTri-9 Generates Intracellular ROS

Given the recent reports of gold-based chemotherapeutics inducing apoptosis as a result of ROS generation, we investigated the ability of **AuTri-9** to generate intracellular ROS.[36,56−60] Using 2′,7′-dichlorofluorescin diacetate (DCF-DA) a fluorogenic dye, which has its fluorescence activated upon oxidation by ROS species, MDA-MB-231 cells were stained and subjected to **AuTri-9** treatment at 5 μM. ROS levels were measured using flow cytometry (ex. FITC channel) at different time points (15 min, 30 min, and 1 h) (Figure 6). *tert*-Butyl hydroperoxide was used as a positive control (50 μM, 1 h). After a 15 min treatment time with **AuTri-9**, significant increase in ROS levels was observed in comparison to the untreated control group. However, after 30 min and furthermore at 1 h, there was no difference in the ROS increase observed earlier for the 15 min treatment. We attribute the

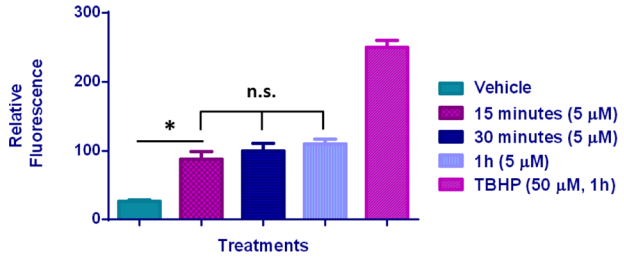

Figure 6. Intracellular ROS accumulation in MDA-MB-231 monitored by DCF-DA fluorescence using FACS. **AuTri-9** was used at a concentration of 5 μM for the designated time points. TBHP was used as a positive control. 1% DMSO was used as the vehicle control. Data are plotted as the mean ± s.d., n = 3, n.s. = not significant, and * $p < 0.01$.

phenomenon to initial oxidative stress on the cells upon exposure to **AuTri-9**. However, since ROS levels do not drastically increase over exposure time, we posit that ROS may not be a major contributor to cell cytotoxicity.

Quantitative Proteomics

Considering previous effects of gold molecules on intracellular thiols, we sought to use quantitative proteomics to deepen our understanding of the potential targets or pathways impacted by **AuTri-9**. We subjected **AuTri-9**-treated MDA-MB-231 cells to TMT-labeled quantitative proteomics and analyzed for differential protein changes compared to vehicle-treated MDA-MB-231 cells. The raw MS files were analyzed and searched against HUMAN protein database based on the species of the samples using Maxquant. Only high confident identified peptides were chosen for downstream protein identification analysis. A quantitative ratio over 1.5 was considered upregulation while quantitative ratio less than 1/1.5 was considered as downregulation. The data revealed significant down regulation of RAS family proteins, specifically GTPases and RAB proteins. More specifically, **AuTri-9** downregulated mitochondria structural proteins (e.g., OPA1, MFN1, and TOM20) without affecting protein content of the OXPHOS machinery and cell metabolism based proteins (including SOD1, SOD2, and NRF2) (Figure 7). Other proteins of interest were also found

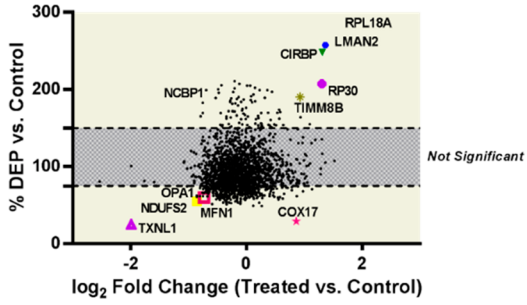

Figure 7. Quantitative proteomics in MDA-MB-231 upon treatment with **AuTri-9** (1 μM, for 12 h).

to be downregulated, such as TXLN-1 (Figure 7), a sulfur containing thioredoxin like protein. Unsurprisingly, downregulation of these proteins is common given the affinity of a soft polarizable metal like gold and the softer nature of sulfur atoms. However, after compilation of significant protein concentration changes, our findings indicated that these compounds could potentially be attacking mitochondria structure rather than cell metabolism. Together, protein

https://dx.doi.org/10.1021/jacsau.1c00051
JACS Au XXXX, XXX, XXX−XXX

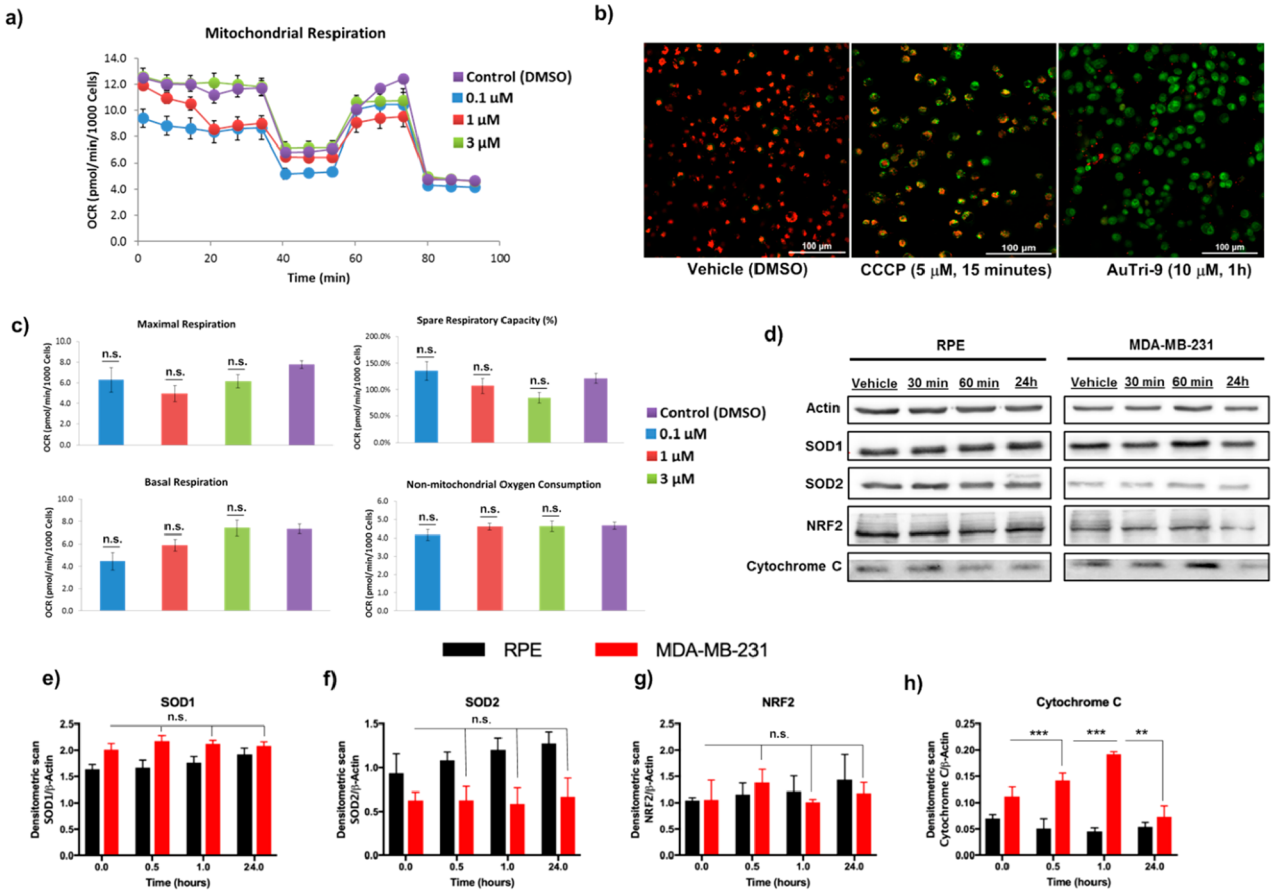

Figure 8. (a) Mitostress test performed in MDA-MB-231 with **AuTri-9** (injected pneumatically). Data are plotted as mean ± s.d. n = 8. (b) Metabolic parameters derived from the Mitostress test. Data are plotted as mean ± s.d. n = 8. (c) JC-1 fluorimetric determination of MMP in MDA-MB-231 using **AuTri-9**. Images are representative of 3 separate replicates. (d) Immunoblotting of SOD1, SOD2, NRF2, and cytochrome C. Full blots can be found in the Supporting Information. (e–h) Representative quantitative protein content of SOD1, SOD2, NRF2, and cytochrome C respectively, n = 5.

studies corroborate the rapid disruption of mitochondrial structure induced by **AuTri-9**.

Cellular Metabolism Remains Unaffected Upon Treatment with AuTri-9

To fully understand the mechanism of action, knowing that mitochondrial based proteins were modulated, we sought to analyze the effect of **AuTri-9** treatment on metabolism. Compounds that disrupt the electron transport chain (ETC) are potent inhibitors of cell metastasis as cancer cells hijack OXPHOS machinery to support growth.[61] First, we treated cells with **AuTri-9** via pneumatic injection in a mitostress assay using Seahorse XF96 and analyzed the changes in OCR (oxygen consumption rate) over time. Next, known OXPHOS inhibitors were injected: oligomycin, a complex V inhibitor, to view the basal OCR; FCCP, an uncoupler used to observe the maximum OCR, and rotenone/antimycin A, a complex I/III inhibitor to completely shut down the ETC (Figure 8a). To our surprise, at concentrations 6 times the IC_{50} of **AuTri-9**, no significant change in OCR was observed after the 90 min experimental protocol. Often, pneumatic injection is preferred over pretreating cells with the agent under investigation to better recapitulate direct metabolic effects instead of cell-death associated events. For example, Gboxin, a known small molecule inhibitor of OXPHOS, induces rapid and irreversible inhibition of overall OCR to demonstrate specificity for mitochondrial respiration.[62] Further evaluation of key metabolic parameters including basal OCR, maximal OCR, spare respiratory capacity, and nonmitochondrial dependent oxygen consumption remain unaltered (Figure 8b). Although OXPHOS is critical for cancer cell proliferation and survival, it is clear that other cell pathways involving mitochondria can be a target for cell death. Next, we treated MDA-MB-231 cells with **AuTri-9** to analyze the mitochondrial membrane polarization (MMP), using a known uncoupler carbonyl cyanide m-chlorophenyl hydrazine (CCCP) as a positive control (Figure 8c). The mitochondrial specific dye JC-1 was used, where green fluorescence represents J-monomers and red fluorescence represents J-aggregates.[63] Interestingly, a stark change in MMP was observed upon treatment in 1 h. This drastic change in MMP suggests that the structural changes observed contribute to depolarization. We then performed immunoblotting of key proteins involved in the OXPHOS machinery. These included SOD1, SOD2, NRF2, and cytochrome C (Figure 8d). These proteins were chosen because SOD1/SOD2 reduces intracellular ROS and their inhibition induces cell death by oxidative stress. Increased NRF2 activity provides defense against mitochondrial toxins. Furthermore, down regulation of NRF2 is found in several mitochondrial based diseases, such as Parkinson's disease.[64] Finally, we evaluated cytochrome C levels as it is released into the cell when a cell receives apoptotic stimuli. Given the key roles, these proteins play in maintaining redox homeostasis,

https://dx.doi.org/10.1021/jacsau.1c00051
JACS Au XXXX, XXX, XXX–XXX

immunoblotting provides concrete evidence of protein level upon treatment. In contrast, upon treatment of both RPE cells and MDA-MB-231 cells, no change in protein levels could be observed. Measurements of integrated density of protein bands was performed using Image Studio Software (version 5.2.5), with background correction calculated using a signal ratio error model. To quantify the protein content (Figure 8e–h), the bands were analyzed with LI-COR and normalized by β-actin levels. Calculations of relative signal were normalized to untreated sample for each set, as indicated. Analysis of the immunoblots showed no significant changes in the proteins examined, suggesting that **AuTri-9** does not interact directly with OXPHOS machinery or key cytosolic proteins that maintain cell redox homeostasis.

Cellular Uptake of AuTri-9 and Mechanism

We, then, sought to understand the uptake mechanism of **AuTri-9** in cells. Understanding the target and uptake pathway is crucial when developing new therapeutic agents or probes. Subcellular localization of therapeutic agents to better understand specific target binding and the affinity a therapeutic has toward certain parts of the cell. This insight helps further elucidate the mechanism of action of therapeutic agents as one can pinpoint the specific binding target. We analyzed gold content in specific cellular fractions including, nucleus, cytoplasm, membranes, and mitochondria. This data revealed that localization of **AuTri-9** was found to occur in the cytoplasm of the cell (Figure 9a). This can be attributed to the

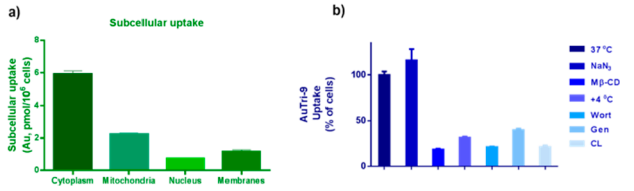

Figure 9. Cellular uptake of **AuTri-9** using GF-AAS in MDA-MB-231. (a) Subcellular uptake of **AuTri-9** in MDA-MB-231 at 1 μM for 6 h. Data are plotted as the mean ± s.d., n = 3. (b) Uptake inhibition using known inhibitors 1 h prior to treatment with **AuTri-9** (1 μM, 6 h). Data are plotted as the mean ± s.d., n = 3.

lipophilicity associated with **AuTri-9**. We observed relatively lower gold uptake in both the nucleus and cellular membranes. The gold compound localized within the mitochondria at >2 pmol/million cells. To determine the potential mechanism of cellular uptake, we first treated MDA-MB-231 with **AuTri-9** to determine the whole cell uptake. Next, we pretreated cells with known uptake inhibitors: sodium azide (NaN_3), which is known to inhibit mitochondrial oxidative phosphorylation and was used as a general inhibitor of energy (ATP)-dependent (active) uptake; chlorpromazine (CL) was utilized as an inhibitor of clathrindependent endocytosis (CDE); b-cyclodextrin (Me-β-CD) and genestein (Gen) were used as inhibitors of clathrin-independent endocytosis (CIE); and wortmannin (Wort) was employed as a known inhibitor of micropinocytosis (Figure 9b). The high cellular uptake of Au with respect to our control when pretreated with NaN_3 shows that OXPHOS is not a key factor in uptake of the compound. This further confirms our hypothesis that these compounds do not directly affect OXPHOS machinery in cancer cells. Other inhibitors collectively show a reduction in Au uptake, indicative of a broad uptake mechanism. Overall, this study illustrates a new way of targeting mitochondria via structural perturbation, rather than direct interaction of OXPHOS machinery.

Preliminary In Vivo Studies of AuTri-9

To determine preliminary in vivo tolerance, we treated female athymic Nu/nude mice with **AuTri-9** at a dose of 10 mg/kg based on gold (every other day, three-times per week, 7×). With known gold agents having a MTD (maximum tolerated dose from 3 to 10 mg/kg and auranofin (12 mg/kg based on gold), 10 mg/kg provided us with a more accurate estimation of overall in vivo toxicity.[65−68] We compared our treatment group to a separate control group of mice that were administered with 85% Kolliphor, 1% DMSO, and 4% PBS (n = 2 mice per group) (Figure 10). We monitored the weight

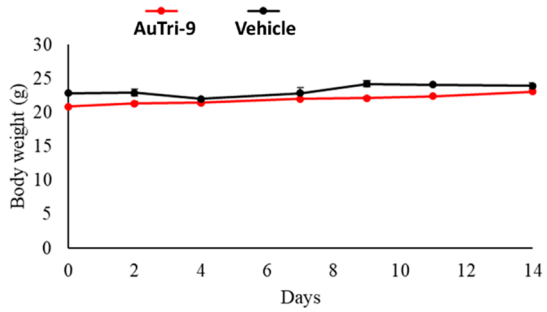

Figure 10. In vivo toxicity as determined by mouse body weight. Female athymic Nu/Nude mice were treated with **AuTri-9** or vehicle control at 10 mg/kg twice a week via intraperitoneal injection. n = 2.

and behavior of the mice every 2 days for signs of toxicity. After a 14-day treatment time, all mice were recorded with no significant change in body weight. This preliminary data suggests that the compound is tolerable in mice, a critical component in further drug/probe development.

CONCLUSION

All together, we have taken advantage of a facile synthetic strategy to access a small library of unique tricoordinate gold(I) complexes. We have demonstrated that this geometry seems to play a critical role in cellular toxicity due to the increase in toxicity over traditional linear gold(I) complexes. These complexes exhibit high in vitro cytotoxicity with a clear improvement based on SAR. Furthermore, the compounds display a >35 times selectivity toward TNBC's over normal lung fibroblasts. Our best candidate displayed promising cytotoxicity in multiple cell lines. With the use of quantitative proteomics, we were able to gather critical information which signaled a mitochondrial driven mechanism. Combined bioenergetics studies revealed no significant effect on bioenergetics; however, a direct change in overall MMP, which suggests a change in mitochondrial dynamics independent from OXPHOS. Electron microscopy revealed significant morphological changes, which are different from traditional cell death pathways, which was further confirmed by immunoblotting of mitochondrial structure proteins. Cellular uptake was then quantified and revealed that **AuTri-9** was taken up into the cell via a broad mechanism and gold content found to be localized in mitochondria. Finally, preliminary in vivo studies suggest that these compounds are potential candidates for further evaluation as **AuTri-9** was tolerated in mice at 10 mg/kg over a two-week period. All of these factors illustrate for the first time, biological utility of tricoordinate

https://dx.doi.org/10.1021/jacsau.1c00051
JACS Au XXXX, XXX, XXX−XXX

gold(I) complexes as mitochondrial probes and anticancer agents.

■ ASSOCIATED CONTENT

Supporting Information

The Supporting Information is available free of charge at https://pubs.acs.org/doi/10.1021/jacsau.1c00051.

All characterization data of the complexes and experimental procedures (PDF)

■ AUTHOR INFORMATION

Corresponding Author

Samuel G. Awuah − *Department of Chemistry and Department of Pharmaceutical Sciences, College of Pharmacy, University of Kentucky, Lexington, Kentucky 40506, United States*; orcid.org/0000-0003-4947-7283; Email: awuah@uky.edu

Authors

R. Tyler Mertens − *Department of Chemistry, University of Kentucky, Lexington, Kentucky 40506, United States*

William C. Jennings − *Department of Chemistry, University of Kentucky, Lexington, Kentucky 40506, United States*

Samuel Ofori − *Department of Chemistry, University of Kentucky, Lexington, Kentucky 40506, United States*

Jong Hyun Kim − *Department of Chemistry, University of Kentucky, Lexington, Kentucky 40506, United States*

Sean Parkin − *Department of Chemistry, University of Kentucky, Lexington, Kentucky 40506, United States*

Gunnar F. Kwakye − *Department of Neuroscience, Oberlin College, Oberlin, Ohio 44074, United States*

Complete contact information is available at: https://pubs.acs.org/10.1021/jacsau.1c00051

Funding

We are grateful to the University of Kentucky and Oberlin College for funding. The authors acknowledge support from the Center for Pharmaceutical Research and Innovation (NIH P20 GM130456) and the Oberlin College Office of Foundation, Government and Corporate Grants (Grant-in-Aid to Gunnar F. Kwakye)

Notes

The authors declare no competing financial interest.

■ ACKNOWLEDGMENTS

We would like to thank all of the facilities at the University of Kentucky who provided support in completion of the experiments detailed in this manuscript. The UK NMR Center supported by NSF (CHE997738) and the UK X-ray facility supported by the MRI program from NSF (CHE-1625732). For the flow cytometry experiments, we would like to thank Greg Bauman PhD (UK Flow Cytometry and Immune Function core supported by the Office of the Vice President of Research, the Markey Cancer Center, and NCI Center Core Support Grant (P30 CA177558). For microscopy, we would like to thank Dr. Thomas Wilkop and Mr. James Schwartz (UK Light Microscopy Core) for their assistance. We would also like to thank Dr. Tomoko Sengoku and Mr. Michael Alstott for the support with our redox metabolism experiments, supported by the shared resources of the University of Kentucky Markey Cancer Center (P30CA177558). We would also like to acknowledge Jim Begley for the preparation of TEM samples, located in the Jacob's Science Building, College of Arts and Science, Lexington, KY. Establishment of prep services was made possible through partial support from the Office of the VPR. TEM analysis was conducted at the electron microscopy center (EMC) which belongs to the National Science Foundation NNCI Kentucky Multiscale Manufacturing and Nano Integration Node, supported by ECCS-1542174.

■ REFERENCES

(1) Mannella, C. A. The relevance of mitochondrial membrane topology to mitochondrial function. *Biochim. Biophys. Acta, Mol. Basis Dis.* **2006**, *1762*, 140−7.

(2) Mishra, P.; Chan, D. C. Metabolic regulation of mitochondrial dynamics. *J. Cell Biol.* **2016**, *212*, 379−387.

(3) Mouli, P. K.; Twig, G.; Shirihai, O. S. Frequency and selectivity of mitochondrial fusion are key to its quality maintenance function. *Biophys. J.* **2009**, *96*, 3509−3518.

(4) Westermann, B. Mitochondrial fusion and fission in cell life and death. *Nat. Rev. Mol. Cell Biol.* **2010**, *11*, 872−84.

(5) van der Bliek, A. M.; Shen, Q.; Kawajiri, S. Mechanisms of Mitochondrial Fission and Fusion. *Cold Spring Harbor Perspect. Biol.* **2013**, *5*, a011072.

(6) Mertens, R. T.; Parkin, S.; Awuah, S. G. Cancer cell-selective modulation of mitochondrial respiration and metabolism by potent organogold(III) dithiocarbamates. *Chem. Sci.* **2020**, *11*, 10465−10482.

(7) Chen, X.; Glytsou, C.; Zhou, H.; Narang, S.; Reyna, D. E.; Lopez, A.; Sakellaropoulos, T.; Gong, Y.; Kloetgen, A.; Yap, Y. S.; Wang, E.; Gavathiotis, E.; Tsirigos, A.; Tibes, R.; Aifantis, I. Targeting Mitochondrial Structure Sensitizes Acute Myeloid Leukemia to Venetoclax Treatment. *Cancer Discovery* **2019**, *9*, 890−909.

(8) Finkelstein, A. E.; Walz, D. T.; Batista, V.; Mizraji, M.; Roisman, F.; Misher, A. Auranofin. New oral gold compound for treatment of rheumatoid arthritis. *Ann. Rheum. Dis.* **1976**, *35*, 251−257.

(9) Nardon, C.; Boscutti, G.; Fregona, D. Beyond platinums: gold complexes as anticancer agents. *Anticancer Res.* **2014**, *34*, 487−92.

(10) Kostova, I. Gold coordination complexes as anticancer agents. *Anti-Cancer Agents Med. Chem.* **2006**, *6*, 19−32.

(11) Kim, J. H.; Reeder, E.; Parkin, S.; Awuah, S. G. Gold(I/III)-Phosphine Complexes as Potent Antiproliferative Agents. *Sci. Rep.* **2019**, *9*, 12335.

(12) Gukathasan, S.; Parkin, S.; Awuah, S. G. Cyclometalated Gold(III) Complexes Bearing DACH Ligands. *Inorg. Chem.* **2019**, *58*, 9326−9340.

(13) Bertrand, B.; Casini, A. A golden future in medicinal inorganic chemistry: the promise of anticancer gold organometallic compounds. *Dalton Trans.* **2014**, *43*, 4209−4219.

(14) Ndagi, U.; Mhlongo, N.; Soliman, M. E. Metal complexes in cancer therapy - an update from drug design perspective. *Drug Des., Dev. Ther.* **2017**, *11*, 599−616.

(15) Mármol, I.; Quero, J.; Rodríguez-Yoldi, M. J.; Cerrada, E. Gold as a Possible Alternative to Platinum-Based Chemotherapy for Colon Cancer Treatment. *Cancers* **2019**, *11*, 780.

(16) Yue, S.; Luo, M.; Liu, H.; Wei, S. Recent Advances of Gold Compounds in Anticancer Immunity. *Front. Chem.* **2020**, *8*, 543.

(17) Hu, D.; Lok, C.-N.; Che, C.-M. Anticancer Gold Compounds. In *Metal-Based Anticancer Agents*; The Royal Society of Chemistry, Cambridge, England, 2019; pp 120−142.

(18) Elie, B. T.; Hubbard, K.; Pechenyy, Y.; Layek, B.; Prabha, S.; Contel, M. Preclinical evaluation of an unconventional ruthenium-gold-based chemotherapeutic: RANCE-1, in clear cell renal cell carcinoma. *Cancer Med.* **2019**, *8*, 4304−4314.

(19) Elie, B. T.; Hubbard, K.; Layek, B.; Yang, W. S.; Prabha, S.; Ramos, J. W.; Contel, M. Auranofin-Based Analogues Are Effective Against Clear Cell Renal Carcinoma In Vivo and Display No

https://dx.doi.org/10.1021/jacsau.1c00051
JACS Au XXXX, XXX, XXX−XXX

Significant Systemic Toxicity. *ACS Pharmac. & Transl. Sci.* **2020**, *3*, 644−654.
(20) Concepción Gimeno, M.; Laguna, A. Gold chemistry with ferrocene derivatives as Ligands. *Gold Bulletin* **1999**, *32*, 90−95.
(21) Gimeno, M. C. Chemistry of Gold. *Modern Supramolecular Gold Chemistry: Gold-Metal Interactions and Applications*; Laguna, A., Ed.; Wiley: Weinheim, Germany 2008.
(22) Crespo, O.; Gimeno, M. C.; Laguna, A.; Jones, P. G. Two-, three- and four-coordinate gold(I) complexes of 1,2-bis-(diphenylphosphino)-1,2-dicarba-closo-dodecaborane. *J. Chem. Soc., Dalton Trans.* **1992**, *10*, 1601−1605.
(23) Visbal, R.; Ospino, I.; López-de-Luzuriaga, J. M.; Laguna, A.; Gimeno, M. C. N-Heterocyclic Carbene Ligands as Modulators of Luminescence in Three-Coordinate Gold(I) Complexes with Spectacular Quantum Yields. *J. Am. Chem. Soc.* **2013**, *135*, 4712−4715.
(24) Jones, G. C. H.; Jones, P. G.; Maddock, A. G.; Mays, M. J.; Vergnano, P. A.; Williams, A. F. Structure and bonding in gold(I) compounds. Part 3. Mössbauer spectra of three-co-ordinate complexes. *J. Chem. Soc., Dalton Trans.* **1977**, *15*, 1440−1443.
(25) Usón, R.; Laguna, A.; Navarro, A.; Parish, R. V.; Moore, L. S. Synthesis and reactivity of perchlorate bis(tetrahydrothiophen)gold-(I). 197Au Mössbauer spectra of three-coordinate gold(I) complexes. *Inorg. Chim. Acta* **1986**, *112*, 205−208.
(26) Navarro, M.; Toledo, A.; Joost, M.; Amgoune, A.; Mallet-Ladeira, S.; Bourissou, D. π Complexes of P∧P and P∧N chelated gold(I). *Chem. Commun.* **2019**, *55*, 7974−7977.
(27) Yang, Y.; Eberle, L.; Mulks, F. F.; Wunsch, J. F.; Zimmer, M.; Rominger, F.; Rudolph, M.; Hashmi, A. S. K. Trans Influence of Ligands on the Oxidation of Gold(I) Complexes. *J. Am. Chem. Soc.* **2019**, *141*, 17414−17420.
(28) Kleinhans, G.; Hansmann, M. M.; Guisado-Barrios, G.; Liles, D. C.; Bertrand, G.; Bezuidenhout, D. I. Nucleophilic T-Shaped (LXL)Au(I)-Pincer Complexes: Protonation and Alkylation. *J. Am. Chem. Soc.* **2016**, *138*, 15873−15876.
(29) Luong, L. M. C.; Aristov, M. M.; Adams, A. V.; Walters, D. T.; Berry, J. F.; Olmstead, M. M.; Balch, A. L. Unsymmetrical Coordination of Bipyridine in Three-Coordinate Gold(I) Complexes. *Inorg. Chem.* **2020**, *59*, 4109−4117.
(30) López-de-Luzuriaga, J. M.; Monge, M.; Olmos, M. E.; Rodríguez-Castillo, M.; Soldevilla, I.; Sundholm, D.; Valiev, R. R. Perhalophenyl Three-Coordinate Gold(I) Complexes as TADF Emitters: A Photophysical Study from Experimental and Computational Viewpoints. *Inorg. Chem.* **2020**, *59*, 14236−14244.
(31) Joost, M.; Zeineddine, A.; Estévez, L.; Mallet-Ladeira, S.; Miqueu, K.; Amgoune, A.; Bourissou, D. Facile Oxidative Addition of Aryl Iodides to Gold(I) by Ligand Design: Bending Turns on Reactivity. *J. Am. Chem. Soc.* **2014**, *136*, 14654−14657.
(32) Zeineddine, A.; Rekhroukh, F.; Sosa Carrizo, E. D.; Mallet-Ladeira, S.; Miqueu, K.; Amgoune, A.; Bourissou, D. Isolation of a Reactive Tricoordinate α-Oxo Gold Carbene Complex. *Angew. Chem., Int. Ed.* **2018**, *57*, 1306−1310.
(33) McKeage, M. J.; Berners-Price, S. J.; Galettis, P.; Bowen, R. J.; Brouwer, W.; Ding, L.; Zhuang, L.; Baguley, B. C. Role of lipophilicity in determining cellular uptake and antitumour activity of gold phosphine complexes. *Cancer Chemother. Pharmacol.* **2000**, *46*, 343−350.
(34) Mahepal, S.; Bowen, R.; Mamo, M. A.; Layh, M.; Jansen van Rensburg, C. E. The In Vitro Antitumour Activity of Novel, Mitochondrial-Interactive, Gold-Based Lipophilic Cations. *Met.-Based Drugs* **2008**, 864653.
(35) Vela, L.; Contel, M.; Palomera, L.; Azaceta, G.; Marzo, I. Iminophosphorane−organogold(III) complexes induce cell death through mitochondrial ROS production. *J. Inorg. Biochem.* **2011**, *105*, 1306−1313.
(36) Barnard, P. J.; Berners-Price, S. J. Targeting the mitochondrial cell death pathway with gold compounds. *Coord. Chem. Rev.* **2007**, *251*, 1889−1902.
(37) Hickey, J. L.; Ruhayel, R. A.; Barnard, P. J.; Baker, M. V.; Berners-Price, S. J.; Filipovska, A. Mitochondria-Targeted Chemotherapeutics: The Rational Design of Gold(I) N-Heterocyclic Carbene Complexes That Are Selectively Toxic to Cancer Cells and Target Protein Selenols in Preference to Thiols. *J. Am. Chem. Soc.* **2008**, *130*, 12570−12571.
(38) Baker, M. V.; Barnard, P. J.; Berners-Price, S. J.; Brayshaw, S. K.; Hickey, J. L.; Skelton, B. W.; White, A. H. Cationic, linear Au(i) N-heterocyclic carbene complexes: synthesis, structure and anti-mitochondrial activity. *Dalton Trans.* **2006**, *30*, 3708−3715.
(39) Che, C.-M.; Sun, R. W.-Y. Therapeutic applications of gold complexes: lipophilic gold(III) cations and gold(I) complexes for anti-cancer treatment. *Chem. Commun.* **2011**, *47*, 9554−9560.
(40) Zhang, C.; Fortin, P.-Y.; Barnoin, G.; Qin, X.; Wang, X.; Fernandez Alvarez, A.; Bijani, C.; Maddelein, M.-L.; Hemmert, C.; Cuvillier, O.; Gornitzka, H. An Artemisinin-Derivative−(NHC)Gold-(I) Hybrid with Enhanced Cytotoxicity through Inhibition of NRF2 Transcriptional Activity. *Angew. Chem., Int. Ed.* **2020**, *59*, 12062−12068.
(41) Mertens, R. T.; Kim, J. H.; Jennings, W. C.; Parkin, S.; Awuah, S. G. Revisiting the reactivity of tetrachloroauric acid with N,N-bidentate ligands: structural and spectroscopic insights. *Dalton Trans.* **2019**, *48*, 2093−2099.
(42) Johnstone, T. C.; Park, G. Y.; Lippard, S. J. Understanding and improving platinum anticancer drugs—Phenanthriplatin. *Anticancer Res.* **2014**, *34*, 471−476.
(43) Shen, D.-W.; Pouliot, L. M.; Hall, M. D.; Gottesman, M. M. Cisplatin resistance: a cellular self-defense mechanism resulting from multiple epigenetic and genetic changes. *Pharmacol. Rev.* **2012**, *64*, 706−721.
(44) Damia, G.; Broggini, M. Platinum Resistance in Ovarian Cancer: Role of DNA Repair. *Cancers* **2019**, *11*, 119.
(45) Mylavarapu, S.; Das, A.; Roy, M. Role of BRCA Mutations in the Modulation of Response to Platinum Therapy. *Front. Oncol.* **2018**, *8*, 16−16.
(46) Wang, F.-Y.; Tang, X.-M.; Wang, X.; Huang, K.-B.; Feng, H.-W.; Chen, Z.-F.; Liu, Y.-N.; Liang, H. Mitochondria-targeted platinum(II) complexes induce apoptosis-dependent autophagic cell death mediated by ER-stress in A549 cancer cells. *Eur. J. Med. Chem.* **2018**, *155*, 639−650.
(47) Erxleben, A. Mitochondria-Targeting Anticancer Metal Complexes. *Curr. Med. Chem.* **2019**, *26*, 694−728.
(48) Tong, K.-C.; Lok, C.-N.; Wan, P.-K.; Hu, D.; Fung, Y. M. E.; Chang, X.-Y.; Huang, S.; Jiang, H.; Che, C.-M. An anticancer gold(III)-activated porphyrin scaffold that covalently modifies protein cysteine thiols. *Proc. Natl. Acad. Sci. U. S. A.* **2020**, *117*, 1321−1329.
(49) Dixon, S. J.; Lemberg, K. M.; Lamprecht, M. R.; Skouta, R.; Zaitsev, E. M.; Gleason, C. E.; Patel, D. N.; Bauer, A. J.; Cantley, A. M.; Yang, W. S.; Morrison, B.; Stockwell, B. R. Ferroptosis: An Iron-Dependent Form of Nonapoptotic Cell Death. *Cell* **2012**, *149*, 1060−1072.
(50) Wasilewski, M.; Scorrano, L. The changing shape of mitochondrial apoptosis. *Trends Endocrinol. Metab.* **2009**, *20*, 287−94.
(51) Schleiff, E.; Turnbull, J. L. Functional and Structural Properties of the Mitochondrial Outer Membrane Receptor Tom20. *Biochemistry* **1998**, *37*, 13043−13051.
(52) Qi, Y.; Yan, L.; Yu, C.; Guo, X.; Zhou, X.; Hu, X.; Huang, X.; Rao, Z.; Lou, Z.; Hu, J. Structures of human mitofusin 1 provide insight into mitochondrial tethering. *J. Cell Biol.* **2016**, *215*, 621−629.
(53) Chen, H.; Detmer, S. A.; Ewald, A. J.; Griffin, E. E.; Fraser, S. E.; Chan, D. C. Mitofusins Mfn1 and Mfn2 coordinately regulate mitochondrial fusion and are essential for embryonic development. *J. Cell Biol.* **2003**, *160*, 189−200.
(54) Gandre-Babbe, S.; van der Bliek, A. M. The Novel Tail-anchored Membrane Protein Mff Controls Mitochondrial and Peroxisomal Fission in Mammalian Cells. *Mol. Biol. Cell* **2008**, *19*, 2402−2412.
(55) Olichon, A.; Baricault, L.; Gas, N.; Guillou, E.; Valette, A.; Belenguer, P.; Lenaers, G. Loss of OPA1 Perturbates the

https://dx.doi.org/10.1021/jacsau.1c00051
JACS Au XXXX, XXX, XXX−XXX

Mitochondrial Inner Membrane Structure and Integrity, Leading to Cytochrome c Release and Apoptosis. *J. Biol. Chem.* **2003**, *278*, 7743−7746.
(56) Milacic, V.; Chen, D.; Ronconi, L.; Landis-Piwowar, K. R.; Fregona, D.; Dou, Q. P. A Novel Anticancer Gold(III) Dithiocarbamate Compound Inhibits the Activity of a Purified 20S Proteasome and 26S Proteasome in Human Breast Cancer Cell Cultures and Xenografts. *Cancer Res.* **2006**, *66*, 10478.
(57) Vela, L.; Contel, M.; Palomera, L.; Azaceta, G.; Marzo, I. Iminophosphorane-organogold(III) complexes induce cell death through mitochondrial ROS production. *J. Inorg. Biochem.* **2011**, *105*, 1306−1313.
(58) Mármol, I.; Virumbrales-Muñoz, M.; Quero, J.; Sánchez-de-Diego, C.; Fernández, L.; Ochoa, I.; Cerrada, E.; Yoldi, M. J. R. Alkynyl gold(I) complex triggers necroptosis via ROS generation in colorectal carcinoma cells. *J. Inorg. Biochem.* **2017**, *176*, 123−133.
(59) Zhang, C.; Maddelein, M.-L.; Wai-Yin Sun, R.; Gornitzka, H.; Cuvillier, O.; Hemmert, C. Pharmacomodulation on Gold-NHC complexes for anticancer applications − is lipophilicity the key point? *Eur. J. Med. Chem.* **2018**, *157*, 320−332.
(60) Ganga Reddy, V.; Srinivasa Reddy, T.; Privér, S. H.; Bai, Y.; Mishra, S.; Wlodkowic, D.; Mirzadeh, N.; Bhargava, S. Synthesis of Gold(I) Complexes Containing Cinnamide: In Vitro Evaluation of Anticancer Activity in 2D and 3D Spheroidal Models of Melanoma and In Vivo Angiogenesis. *Inorg. Chem.* **2019**, *58*, 5988−5999.
(61) Molina, J. R.; Sun, Y.; Protopopova, M.; Gera, S.; Bandi, M.; Bristow, C.; McAfoos, T.; Morlacchi, P.; Ackroyd, J.; Agip, A.-N. A.; Al-Atrash, G.; Asara, J.; Bardenhagen, J.; Carrillo, C. C.; Carroll, C.; Chang, E.; Ciurea, S.; Cross, J. B.; Czako, B.; Deem, A.; Daver, N.; de Groot, J. F.; Dong, J.-W.; Feng, N.; Gao, G.; Gay, J.; Do, M. G.; Greer, J.; Giuliani, V.; Han, J.; Han, L.; Henry, V. K.; Hirst, J.; Huang, S.; Jiang, Y.; Kang, Z.; Khor, T.; Konoplev, S.; Lin, Y.-H.; Liu, G.; Lodi, A.; Lofton, T.; Ma, H.; Mahendra, M.; Matre, P.; Mullinax, R.; Peoples, M.; Petrocchi, A.; Rodriguez-Canale, J.; Serreli, R.; Shi, T.; Smith, M.; Tabe, Y.; Theroff, J.; Tiziani, S.; Xu, Q.; Zhang, Q.; Muller, F.; DePinho, R. A.; Toniatti, C.; Draetta, G. F.; Heffernan, T. P.; Konopleva, M.; Jones, P.; Di Francesco, M. E.; Marszalek, J. R. An inhibitor of oxidative phosphorylation exploits cancer vulnerability. *Nat. Med.* **2018**, *24*, 1036−1046.
(62) Shi, Y.; Lim, S. K.; Liang, Q.; Iyer, S. V.; Wang, H.-Y.; Wang, Z.; Xie, X.; Sun, D.; Chen, Y.-J.; Tabar, V.; Gutin, P.; Williams, N.; De Brabander, J. K.; Parada, L. F. Gboxin is an oxidative phosphorylation inhibitor that targets glioblastoma. *Nature* **2019**, *567*, 341−346.
(63) Perelman, A.; Wachtel, C.; Cohen, M.; Haupt, S.; Shapiro, H.; Tzur, A. JC-1: Alternative excitation wavelengths facilitate mitochondrial membrane potential cytometry. *Cell Death Dis.* **2012**, *3*, e430−e430.
(64) Holmström, K. M.; Kostov, R. V.; Dinkova-Kostova, A. T. The multifaceted role of Nrf2 in mitochondrial function. *Curr. Opin Toxicol* **2016**, *1*, 80−91.
(65) Mirabelli, C. K.; Johnson, R. K.; Sung, C. M.; Faucette, L.; Muirhead, K.; Crooke, S. T. Evaluation of the in vivo antitumor activity and in vitro cytotoxic properties of auranofin, a coordinated gold compound, in murine tumor models. *Cancer Res.* **1985**, *45*, 32−9.
(66) Fernández-Gallardo, J.; Elie, B. T.; Sadhukha, T.; Prabha, S.; Sanaú, M.; Rotenberg, S. A.; Ramos, J. W.; Contel, M. Heterometallic titanium−gold complexes inhibit renal cancer cells in vitro and in vivo. *Chem. Sci.* **2015**, *6*, 5269−5283.
(67) Zou, T.; Lum, C. T.; Lok, C.-N.; Zhang, J.-J.; Che, C.-M. Chemical biology of anticancer gold(III) and gold(I) complexes. *Chem. Soc. Rev.* **2015**, *44*, 8786−8801.
(68) Walther, W.; Dada, O.; O'Beirne, C.; Ott, I.; Sanchez-Sanz, G.; Schmidt, C.; Werner, C.; Zhu, X.; Tacke, M. In Vitro and In Vivo Investigations into the Carbene Gold Chloride and Thioglucoside Anticancer Drug Candidates NHC-AuCl and NHC-AuSR. *Lett. Drug Design Discovery* **2016**, *14*, 125−134.

https://dx.doi.org/10.1021/jacsau.1c00051
JACS Au XXXX, XXX, XXX−XXX